

ANALYSIS AND DESIGN OF COMMON-DIODE TAPPED-INDUCTOR PWM BUCK CONVERTER IN CCM

Nisha Kondrath and Marian K. Kazimierczuk
Wright State University

Abstract: The analysis of common-diode tapped-inductor (diode-to-tap) PWM buck converter operating in CCM is presented. Considering the circuit operations in two different time intervals, the idealized voltage and current waveforms of the circuit components are obtained. Expressions for dc voltage transfer function and component stresses are derived. A design example is presented and is validated using Saber simulations.

Key Words: PWM buck converter, common-diode tapped-inductor, diode-to-tap converter, dc voltage transfer function, switching component stresses.

I. INTRODUCTION

Different tapped-inductor configurations of dc-dc PWM converters are presented in [1]-[9]. Compared to conventional PWM converters, the converters with tapped-inductor configurations permit the duty cycle to be adjusted to values which are neither close to 0 nor close to 1. Furthermore, a better utilization of switching and passive components can be achieved. Also, multiple outputs are possible [8].

The purpose of this paper is to provide an extension to the previous work published in [2]-[4] by presenting the analysis and design of the common-diode tapped-inductor PWM buck converter operating in continuous conduction mode (CCM). This circuit is also known as diode-to-tap buck converter [3], [4]. The idealized voltage and current waveforms of the circuit components are derived by considering the circuit operation in two different time intervals. The dc voltage transfer function is derived by applying volt-second balance to the tapped-inductor voltage waveform. Also, the voltage stresses as well as the current stresses on the switching devices are obtained. Using the analysis, a common-diode tapped-inductor buck converter for the given specifications is designed and the design is validated using Saber simulations.

In Section II, the circuit operation of the common-diode tapped-inductor buck converter operating in the CCM is discussed and the ideal voltage as well as current waveforms associated with each component are obtained. The DC voltage transfer function of the converter in

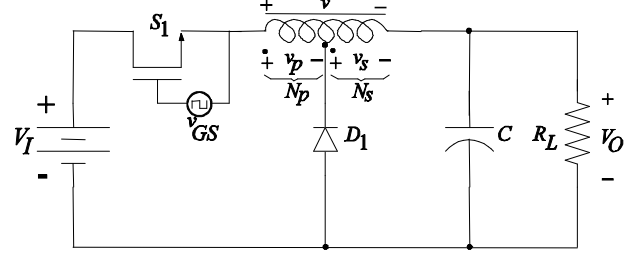


Figure 1. Circuit of common-diode tapped-inductor PWM buck converter.

CCM mode is derived and the stresses associated with each switching component are obtained in Sections III and IV, respectively. The design of the converter is presented in Section V. In Sections VI and VII, the validation using Saber simulations as well as the conclusions are presented.

II. CIRCUIT OPERATION

The common-diode tapped-inductor buck converter circuit is shown in Figure 1. The circuit components include a MOSFET S_1 , a diode D_1 , a tapped-inductor L with a primary inductance of L_p and a secondary inductance of L_s , a filter capacitor C , and a load resistance R_L . The MOSFET S_1 is turned on by a pulse-width modulator output, which in turn decides the duty

cycle of the circuit, $D = \frac{t_{on}}{t_{on} + t_{off}}$, where t_{on} is the time

for which the MOSFET is ON and t_{off} is the time for which the MOSFET is OFF. When $N_p = 0$, the configuration reduces to that of a conventional buck converter. The turns ratio of the tapped inductor is defined as

$$n = \frac{v}{v_s} = \frac{N_p + N_s}{N_s} = 1 + \frac{N_p}{N_s}, \quad (1)$$

where N_p is the number of turns in the primary, N_s is the number of turns in the secondary, v is the voltage across the total number of turns $N = N_p + N_s$, and v_s is the voltage across the secondary of the tapped inductor. Therefore,

$$v_p = \frac{n-1}{n}v \text{ and } v_s = \frac{v}{n}. \quad (2)$$

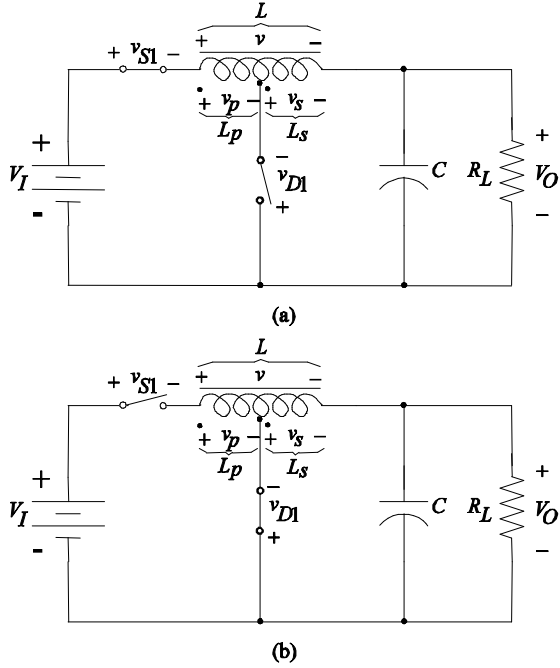


Figure 2. Equivalent circuits in two intervals:
(a) $0 \leq t \leq DT$ (b) $DT \leq t \leq T$.

Now the circuit operation is analyzed by considering two time intervals, the on-time interval t_{on} and the off-time interval t_{off} .

A. On-time Interval $0 \leq t \leq DT$

During this interval, S_1 is ON and D_1 is OFF. The equivalent circuit is shown in Figure 2(a). Since S_1 is closed, the voltage across the switch, $v_{S1} = 0$. The voltage across the total number of turns $N_p + N_s$ is

$$v = V_I - V_O. \quad (3)$$

Also, the voltage across the diode is

$$v_{D1} = -v_s - V_O = -\frac{v}{n} - V_O = -\frac{V_I + (n-1)V_O}{n}. \quad (4)$$

The current through the inductor is given by

$$i_L = \frac{1}{L} \int_0^t v dt + i_L(0) = \frac{V_I - V_O}{L} t + i_L(0). \quad (5)$$

Therefore, the switch current is obtained as

$$i_{S1} = i_L = \frac{V_I - V_O}{L} t + i_L(0) \quad (6)$$

and the diode current is

$$i_{D1} = 0. \quad (7)$$

B. Off-time Interval $DT \leq t \leq T$

In this interval, S_1 is OFF and D_1 is ON. The equivalent circuit is shown in Figure 2(b). The voltage across the diode, $v_{D1} = 0$, and the voltage across the secondary is

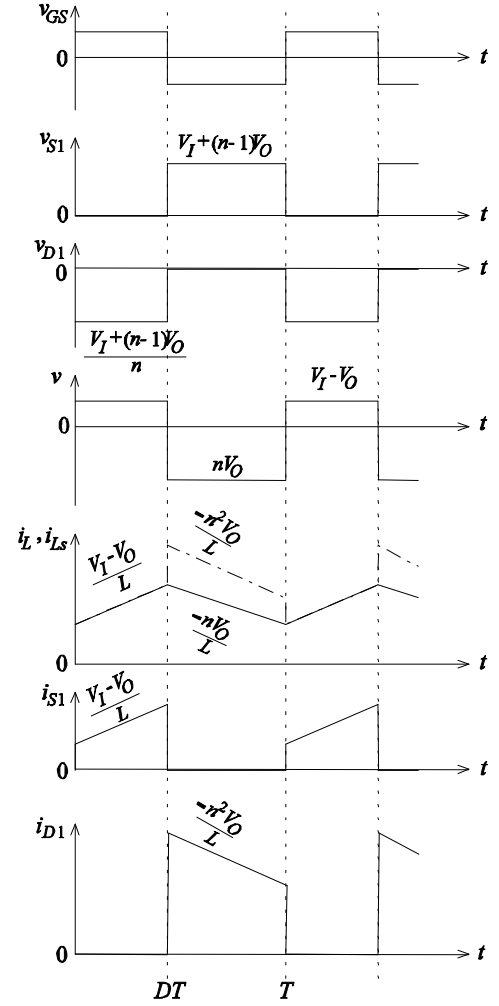


Figure 3. Idealized voltage and current waveforms in common-diode tapped-inductor buck converter in CCM.

$$v_s = -V_O,$$

as the diode is closed in this interval. Thus, the voltage across the total number of turns is

$$v = nv_s = -nV_O. \quad (8)$$

Therefore, the voltage across the switch can be obtained as

$$v_{S1} = V_I - v - V_O = V_I + (n-1)V_O. \quad (9)$$

The current through the secondary of the inductor is obtained as

$$\begin{aligned} i_{Ls} &= ni_L = n \left[\frac{1}{L} \int_{DT}^t v dt + i_L(DT) \right] \\ &= -n^2 \frac{V_O}{L} (t - DT) + ni_L(DT). \end{aligned} \quad (10)$$

Therefore, the diode current is

$$i_{D1} = i_{Ls} = -n^2 \frac{V_O}{L} (t - DT) + ni_L(DT) \quad (11)$$

and the switch current is

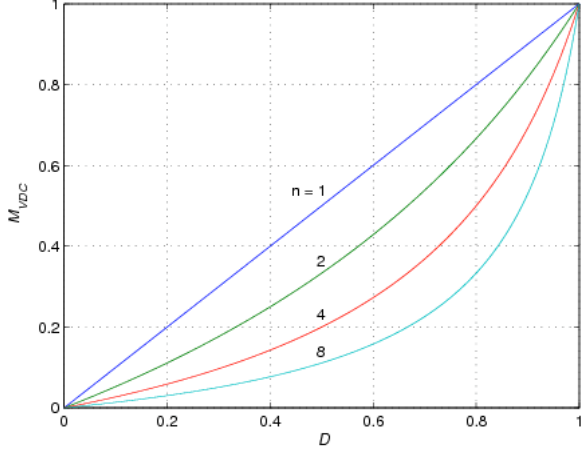


Figure 4. DC voltage transfer function for different values of tapped-inductor turns ratio.

$$i_{S1} = 0. \quad (12)$$

The idealized voltage and current waveforms for one period are obtained using (3)-(12). The obtained voltage and current waveforms for the on-time and off-time intervals are shown in Figure 3.

III. DC VOLTAGE TRANSFER FUNCTION

Using (2) and (3), the voltage across N_s turns, when the switch is ON, is

$$v_s = \frac{V_I - V_O}{n}. \quad (13)$$

Using (2) and (8), when the switch is OFF, is

$$v_s = -V_O. \quad (14)$$

Applying volt-second balance to L_s , we obtain

$$\frac{V_I - V_O}{n} D = V_O (1 - D) \quad (15)$$

Therefore, the dc voltage transfer function is

$$M_{VDC} = \frac{V_O}{V_I} = \frac{D}{D + n(1 - D)}. \quad (16)$$

The variation of the dc voltage transfer function as a function of the duty cycle for different values of turns ratio n is shown in Figure 4. The curve with $n = 1$ corresponds to the conventional buck converter. As n increases, the dc voltage transfer function decreases for a given value of duty cycle. Therefore, compared to regular buck converter, common-diode tapped-inductor buck converter can avoid operation at very low duty cycle to achieve low values of dc voltage transfer function. For example, at $D = 0.5$, $M_{VDC} = 0.5$ and 0.2 for $n = 1$ and 4 , respectively.

IV. SWITCHING COMPONENT STRESSES

A. DC Output Current

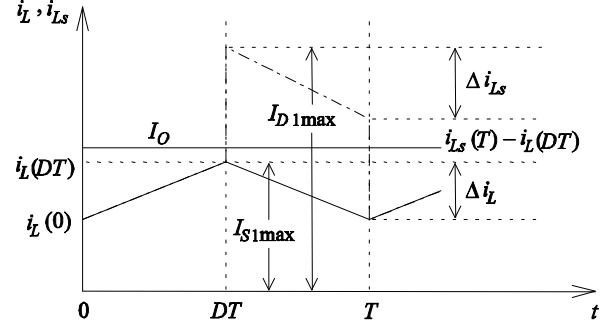


Figure 5. Inductor current and input current waveforms used to obtain the current stresses.

The value of the ripple current in the inductor L can be obtained as

$$\Delta i_L = i_L(DT) - i_L(T) = n \frac{V_O}{L} (T - DT) = n \frac{V_O}{f_s L} (1 - D). \quad (17)$$

The value of the ripple current in the secondary of the inductor L_s can be obtained as

$$\Delta i_{L_s} = i_{L_s}(DT) - i_{L_s}(T) = n^2 \frac{V_O}{f_s L} (1 - D) = n \Delta i_L. \quad (18)$$

The average value of the output current is the average value of the current through the secondary of the inductor L_s . Therefore,

$$\begin{aligned} I_O &= \frac{1}{T} \int_0^T i_{L_s} dt = \frac{1}{T} \left\{ \int_0^{DT} \left[\frac{V_I - V_O}{L} t + i_L(0) \right] dt \right. \\ &\quad \left. + \int_{DT}^T \left[-n^2 \frac{V_O}{L} (t - DT) + n i_L(DT) \right] dt \right\} \\ &= D \left[\frac{V_I - V_O}{2L} DT + i_L(0) \right] \\ &\quad + (1 - D) \left[-n^2 \frac{V_O}{2L} (T - DT) + n i_L(DT) \right] \\ &= D \left[\frac{i_L(DT)}{2} + \frac{i_L(0)}{2} \right] + n(1 - D) \left[\frac{i_L(T)}{2} + \frac{i_L(DT)}{2} \right] \\ &= [D + n(1 - D)] \left[i_L(0) + \frac{\Delta i_L}{2} \right]. \end{aligned} \quad (19)$$

The inductor currents and the input current waveforms are shown in Figure 5.

B. MOSFET Stresses

Using (9), the voltage stress for S_1 is given by

$$V_{S1max} = V_{Imax} + (n - 1)V_O. \quad (20)$$

From Figures 3 and 5 and using (19), the current stress on S_1 can be obtained as

$$I_{S1\max} = i_L(0)_{\max} + \Delta i_{L\max} = i_L(0)_{\max} + \frac{\Delta i_{L\max}}{2} + \frac{\Delta i_{L\max}}{2}$$

$$= \frac{I_{O\max}}{D_{\min} + n(1 - D_{\min})} + n \frac{V_O}{2f_s L} (1 - D_{\min}). \quad (21)$$

Compared to the conventional buck converter, the voltage stress across the MOSFET in a tapped inductor common-diode buck converter increases where as the current stress in the MOSFET decreases.

C. Diode Stresses

Using (4), the voltage stress for D_1 is given by

$$V_{D1\max} = \frac{V_{I\max} + (n-1)V_O}{n} = \frac{V_{S1\max}}{n}. \quad (22)$$

From Figs. 3 and 5, the maximum current flows through D_1 at $t = DT$. Therefore,

$$I_{D1\max} = i_{L_s}(DT). \quad (23)$$

Using (10) and (18), the current through L_s at $t = DT$ is obtained as

$$i_{L_s}(DT) = n i_L(DT) = n [i_L(0)_{\max} + \Delta i_{L\max}] \quad (24)$$

Thus, the current stress on D_1 can be obtained as

$$I_{D1\max} = n I_{S1\max}$$

$$= n \left[\frac{I_{O\max}}{D_{\min} + n(1 - D_{\min})} + n \frac{V_O}{2f_s L} (1 - D_{\min}) \right]. \quad (25)$$

By using a tapped-inductor common-diode buck converter, the voltage stress across the diode can be decreased from that in a conventional buck converter. However, the current stress in the diode increases.

V. DESIGN EXAMPLE

A common-diode tapped-inductor buck converter with input voltage $V_I = 24 \pm 4$ V, output voltage $V_O = 8$ V, output current $I_O = 0.1$ to 1 A, ripple voltage $V_r = 1\%$ of output voltage, and switching frequency $f_s = 100$ kHz is designed as follows:

For a conventional buck converter, the duty cycle $D = \frac{V_O}{V_I}$. Therefore, the maximum duty cycle is

$$D_{\max} = \frac{V_O}{V_{I\min}} = \frac{8}{20} = 0.4,$$

the nominal duty cycle is

$$D_{nom} = \frac{V_O}{V_{I\max}} = \frac{8}{24} = 0.333,$$

and the minimum duty cycle is

$$D_{\min} = \frac{V_O}{V_{I\max}} = \frac{8}{28} = 0.286.$$

Therefore, the range of duty cycle required to provide the required dc voltage transfer function in a conventional buck converter is $< 0.286, 0.4 >$.

The maximum load resistance is

$$R_{L\max} = \frac{V_O}{I_{O\min}} = \frac{8}{0.1} = 80 \Omega$$

and the minimum load resistance is

$$R_{L\min} = \frac{V_O}{I_{O\max}} = \frac{8}{1} = 8 \Omega.$$

A. Value of Total Inductance L

The minimum value of inductance required for the converter to remain in continuous conduction mode [7],[10] is given by

$$L_{\min} = \frac{R_{L\max}(1 - D_{\min})}{2f_s} = \frac{80(1 - 0.286)}{2 \times 10^5} = 286 \mu\text{H}.$$

Choose $L = 301 \mu\text{H}$.

B. Value of Primary Inductance L_p and Secondary Inductance L_s

Assume turns ratio,

$$n = \frac{N_p + N_s}{N_s} = 1 + \frac{N_p}{N_s} = 2.$$

We know, $L \propto N^2$ and $L_s \propto N_s^2$. Thus,

$$\frac{L}{L_s} = \left(\frac{N}{N_s} \right)^2 = n^2 = 4 \text{ and } L_p = L_s.$$

Therefore,

$$L_p = L_s = \frac{L}{4} = \frac{301}{4} = 75.25 \mu\text{H}.$$

C. Value of Capacitance C

The maximum value of the ripple current through the capacitor [7],[10] is

$$\Delta i_{L\max} = \frac{V_O(1 - D_{\min})}{f_s L} = \frac{8(1 - 0.286)}{10^5 \times 301 \times 10^{-6}} = 0.19 \text{ A}.$$

The maximum value of the ESR of the capacitor is

$$r_{C\max} = \frac{V_r}{\Delta i_{L\max}} = \frac{0.01 \times 8}{0.19} = 0.0421 \Omega.$$

Choose $r_C = 0.039 \Omega$. Therefore, the value of capacitance required is

$$C_{\min} = \max \left(\frac{D_{\max}}{2f_s r_C}, \frac{1 - D_{\min}}{2f_s r_C} \right)$$

$$= \max \left(\frac{0.4}{2 \times 10^5 \times 0.039}, \frac{1 - 0.286}{2 \times 10^5 \times 0.039} \right) = 91.67 \mu\text{F}.$$

Pick $C = 100 \mu\text{F}$.

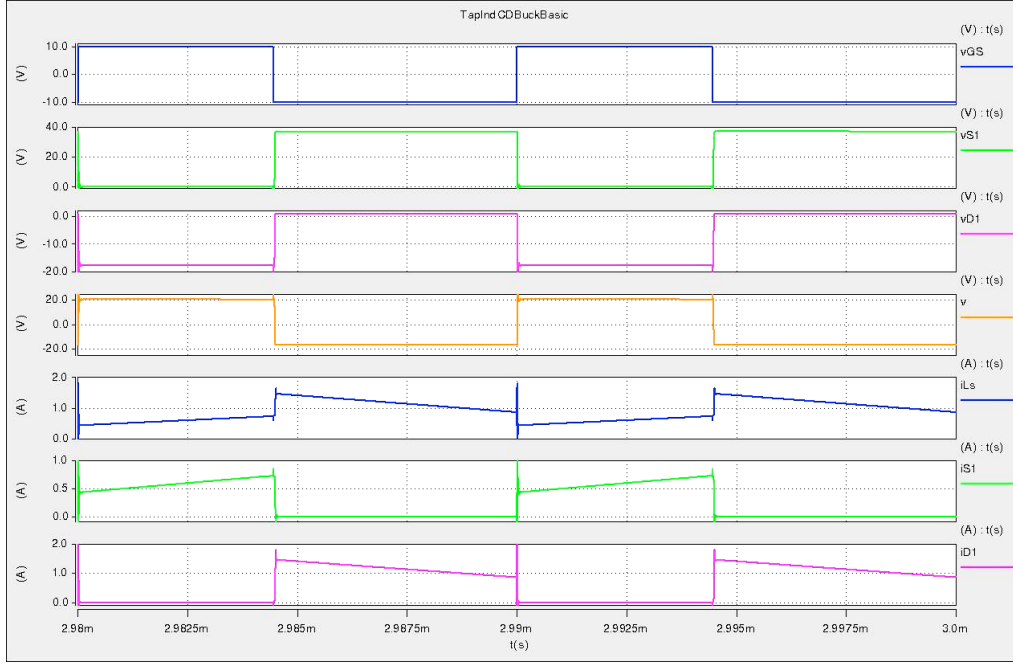


Figure 6: Voltage and current waveforms with $k = 1$ obtained from Saber simulations.

D. Selection of MOSFET

Using (20) and (21), the voltage stress on the MOSFET is

$$V_{S1\max} = V_{I\max} + (n-1)V_O = 28 + (2-1)8 = 36 \text{ V}$$

and the current stress on the MOSFET is

$$\begin{aligned} I_{S1\max} &= \frac{I_{O\max}}{D_{\min} + n(1-D_{\min})} + n \frac{V_O}{2f_s L} (1-D_{\min}) \\ &= \frac{1}{0.286 + 2(1-0.286)} + 2 \times \frac{8(1-0.286)}{2 \times 10^5 \times 301 \times 10^{-6}} \\ &= 0.773 \text{ A.} \end{aligned}$$

Select International Rectifier N-channel power MOSFET IRF530 with $V_{DSS} = 100 \text{ V}$, $I_D = 14 \text{ A}$, and $r_{DS(on)} = 0.16 \Omega$.

E. Selection of Diode

Using (22) and (23), the voltage and current stresses on the diode are

$$V_{D1\max} = \frac{V_{S1\max}}{n} = \frac{36}{2} = 18 \text{ V}$$

and

$$I_{D1\max} = nI_{S1\max} = 2 \times 0.773 = 1.546 \text{ A,}$$

respectively. Select Semiconductor ultrafast rectifier diode MUR820 with $V_R = 200 \text{ V}$ and $I_F = 8 \text{ A}$.

VI. SIMULATION RESULTS

The common-diode designed tapped-inductor buck

converter with $V_I = 28 \text{ V}$, $I_O = 1 \text{ A}$, and $D = 0.445$ was simulated using Saber Sketch. Using (16), the range of duty cycle required to obtain the required dc voltage transfer function using the tapped inductor configuration is obtained as $< 0.445, 0.571 >$. The Saber models for the selected components were obtained from the manufacturers.

The voltage and current waveforms in the MOSFET S_1 , the diode D_1 , voltage waveform in the total inductance L , and the current waveform in the secondary of the coupled inductor L_s with a coupling coefficient of $k = 1$ are shown in Figure 6. As seen from the figure, the waveforms agree with the idealized waveforms shown in Figure 3. But, for all practical applications, it is impossible to have a unity coupling coefficient due to the leakage inductance of the transformer. Therefore, the coupling coefficient of the tapped inductor was chosen to be $k = 0.998$. The voltage and current waveforms obtained with $k = 0.998$ is shown in Figure 7.

As seen in Figure 7, the voltage and current waveforms across the MOSFET, the diode, and the inductor exhibited ringing at the switching transitions. This ringing was due to the presence of the leakage inductance in the tapped-inductor and results in higher voltage as well as current stresses in the switching components. This ringing may be reduced by active or passive clamping to improve the performance of the converter.

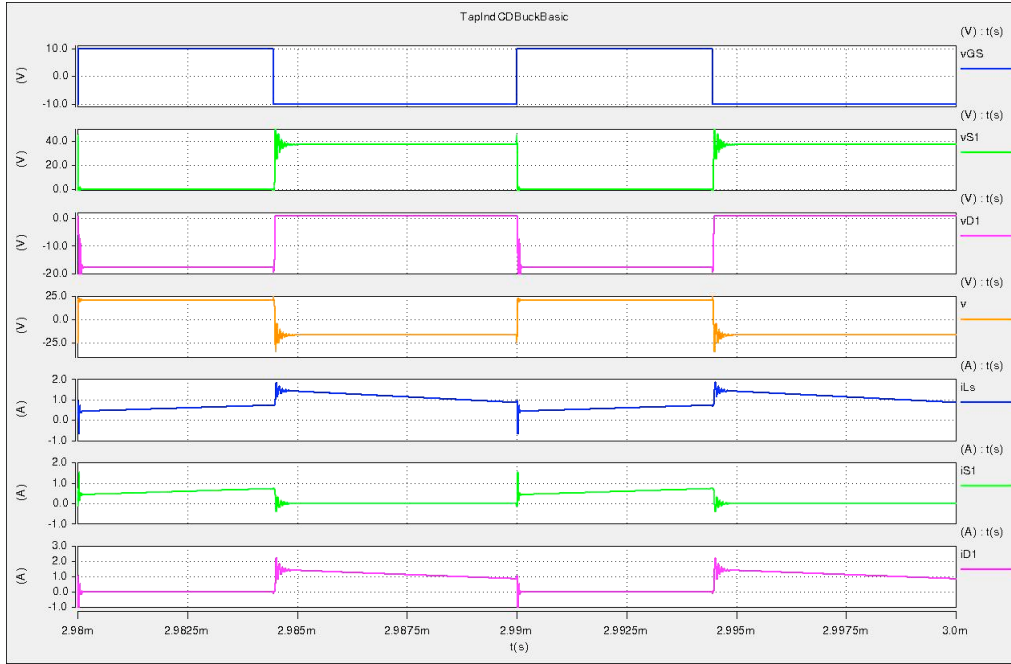


Figure 7: Voltage and current waveforms with $k = 0.998$ obtained from Saber simulations.

VII. CONCLUSIONS

The common-diode tapped-inductor buck converter circuit has been analyzed and the idealized current and voltage waveforms in the switching components as well as in the coupled inductor were obtained. Expressions for the dc voltage transfer function and the component stresses were derived using the obtained idealized inductor voltage and current waveforms. A design example has been presented and has been validated using Saber Sketch simulations.

At a given value of duty cycle, the dc voltage transfer function values of common-diode tapped-inductor buck converter were lower than that of the classical buck converter. This makes it possible to avoid very low values of duty cycle to obtain lower values of dc voltage gain. It was also found that, when compared to the conventional buck converter, the voltage stress on the MOSFET increases and that on the diode decreases as the turns ratio n increases. However, the current stress on the MOSFET decreases and that on the diode increases with increase in n , compared to the conventional configuration. The converter may have multiple outputs due to the presence of coupled tapped-inductor.

Even though the Saber simulations with $k = 1$ agreed with the idealized waveforms, with $k < 1$, they revealed the presence of ringing in all the voltage and current waveforms during transitions due to the leakage inductance of the tapped inductor, thereby increasing the voltage and current stresses on the components even further. Therefore, to improve the performance of the

converter and to reduce the stresses on the switching components it is necessary to design a tapped inductor with high coupling coefficient. This ringing may also be reduced using active or passive clamping to improve the performance of the converter as well as to reduce the stresses.

REFERENCES

1. R. D. Middlebrook, "A continuous model for the tapped-inductor boost converter," *IEEE Power Electronics Specialists Conference (PESC) Record*, pp. 55-71, 1975.
2. R. D. Middlebrook and S. Cuk, "Coupled inductor and other extensions of a new optimum topology switching dc-dc converter," *IEEE IAS Annual Meeting*, pp. 1110-1126, 1977.
3. D. A. Grant and Y. Darroman, "Watkins-Johnson converter completes tapped inductor converter matrix," *Electron. Lett.*, vol. 39, no. 3, pp. 271-272, Feb. 2003.
4. D. A. Grant and Y. Darroman, "Extending the tapped-inductor DC-to-DC converter family," *Electron. Lett.*, vol. 37, no. 3, pp. 145-145, 2001.
5. Jong-Hu Park and B. H. Cho, "The zero voltage switching (ZVS) critical conduction mode (CRM) buck converter with tapped-inductor," *IEEE Trans. Power Electron.*, vol. 20, no. 4, pp. 762-774, July 2005.

6. F. A. Himmelstoss and P. A. Wurm, "Simple bi-directional dc-to-dc converters with high input to output voltage ratio," *17th European Photovoltaic Solar Energy Conference and Exhibition*, Oct. 2001.
7. N. Das and M. K. Kazimierczuk, "Power losses and efficiency of buck PWM DC-DC power converter," *Electrical Insulation Conference and Electrical Manufacturing Expo*, Indianapolis, IN, Oct. 23-26, 2005.
8. Y. Darroman and A. Ferre, "42-V/3-V Watkins-Johnson converter for automotive use," *IEEE Trans. Power Electron.*, vol. 21, no. 3, pp. 592-602, May 2006.
9. N. Kondrath and M. K. Kazimierczuk, "DC voltage transfer function and component stresses of common-diode tapped inductor PWM boost converter," *Electrical Insulation Conference and Electrical Manufacturing Expo*, Orlando, FL, Nov. 3-5, 2008.
10. M. K. Kazimierczuk, *Pulse-width modulated dc-dc power converters*, Chichester, UK: John Wiley & Sons, Ltd, 2008.

Nisha Kondrath received her B.Tech. and M. S. degrees in electrical engineering from Mahatma Gandhi University (MGU), Kerala, India and Wright State University (WSU), Dayton, Ohio, in 2002 and 2005, respectively. She is currently pursuing the PhD degree at WSU and is also working as a research assistant in the Department of Electrical Engineering. Her areas of research interest are in power electronics, high frequency PWM dc-dc converters, power semiconductors, and magnetics. Ms. Kondrath is a member of Tau Beta Pi and Electrical Manufacturing and Coil Winding Association, USA.

Marian K. Kazimierczuk received the M.S., and Ph.D., and D.Sci. degrees in electronics engineering from the Department of Electronics, Technical University of Warsaw, Warsaw, Poland, in 1971, and 1978, and 1984, respectively. He is currently a Professor of Electrical Engineering at Wright State University, Dayton, OH. His areas of research are in high-frequency high-efficiency RF power amplifiers, resonant and PWM dc/dc power converters, dc/ac inverters, high-frequency rectifiers, modeling and control of converters, high-frequency magnetics, power semiconductor devices, electronic ballasts, RF transmitters, sensors, and superconductivity. He is a Fellow of IEEE and has published more than 230 papers. He is the co-author of the book *Resonant Power Converters*, Wiley, 1995.